JOURNAL OF SPACECRAFT AND ROCKETS
Vol. 40, No. 3, May–June 2003

Compressibility Correction for the Spalart–Allmaras Model in Free-Shear Flows

Renato Paciorri* and Filippo Sabetta†
University of Rome "La Sapienza," 00184 Rome, Italy

A correction of the Spalart–Allmaras turbulence model to account for the compressibility effects in mixing-layer flows is presented. Unlike other corrections proposed for the $K-\varepsilon$ model, the present correction does not need the knowledge of the turbulent Mach number and, therefore, can be applied to those turbulence models, like the Spalart–Allmaras one, which do not integrate directly the turbulent kinetic energy equation. To explore the validity of the proposed correction, four mixing-layer flows and four supersonic backward-facing step flows, covering a wide range of flow conditions, were selected and computed using both the standard and the corrected Spalart–Allmaras model. The analysis of the numerical results and their comparison with the experimental data show that the proposed correction produces a significant improvement of the numerical predictions.

Nomenclature

a	=	sound speed, ms^{-1}
f_1, f_2	=	compressibility calibration functions
K	=	turbulent kinetic energy, $\mathrm{m}^2\mathrm{s}^{-2}$
M	=	Mach number
M_c	=	convective Mach number, $(U_1 - U_2)/(a_1 + a_2)$
M_t	=	turbulent Mach number, $(\sqrt{2K})/a$
Re_x	=	Reynolds number, $\rho U x/\mu$
r	=	freestream velocity ratio, $(U_2)/(U_1)$
U	=	freestream velocity, ms^{-1}
u	=	local velocity, ms^{-1}
x, y	=	Cartesian body axes, m
ΔU	=	velocity difference $U_1 - U_2$, ms^{-1}
Δx, Δy	=	computational mesh unit cell size, m
δ_ω	=	vorticity thickness $(\Delta U)/(\partial u/\partial y)_{\max}$, m
ν	=	kinematic molecular viscosity, $\mathrm{m}^2\mathrm{s}^{-1}$
ν_T	=	kinematic eddy viscosity, $\mathrm{m}^2\mathrm{s}^{-1}$
τ	=	dimensionless shear stress, $\overline{u'v'}\vert_{\max}/\Delta U^2$
ω	=	vorticity, s^{-1}

Subscripts

c	=	compressible
i	=	incompressible
max	=	maximum value
1, 2	=	freestream conditions

Superscripts

$'$	=	fluctuation
-	=	average
~	=	estimate

Introduction

THE fluid compressibility can remarkably modify the behavior of turbulence with respect to the incompressible case. The presence of strong pressure-induceddensity changes adds to the turbulence phenomenology new specific processes and mechanisms, such as new pathways for the energy exchanges, a strong coupling between momentum and energy exchanges, etc., significantly altering the flow behavior. Although the phenomenology of the compressible turbulence is still not completely clear, several important effects produced by compressibility have been identified and investigated. A detailed and up-to-date review about the compressibility and its effects on turbulence can be found in Ref. 1.

A turbulent mixing layer is a flow where the compressibility shows the most visible effects and, therefore, has been largely investigated. Numerous studies[2–6] have highlighted that in a compressible mixing layer 1) the thickness growth rate is reduced with respect to an analogous incompressible mixing layer, 2) the strength of the turbulent shear stresses is reduced, and 3) the fundamental parameter governing the compressibility effects is the convective Mach number M_c.

These alterations of the turbulence behavior inside the mixing layer can play a meaningful role in more complex flows. For instance, in supersonic afterbody flows the flowfield is characterized by the presence of mixing layers separating the low-speed recirculating regions from the high-speed stream. The turbulent flows inside these mixing layers are strongly influenced by the compressibility effects, and the whole structure of the recirculating region is altered. As shown in Ref. 7, the modifications produced by compressibility inside the mixing layer affect the size of the separated regions and, consequently, the afterbody drag. Several numerical studies[7–10] have confirmed that the addition of a compressibility correction in the turbulence model significantly improves the afterbody drag estimate of the numerical simulations.

Modified turbulence models, which account for the flow compressibility, were developed[11,12] from the $K-\varepsilon$ model. In both of these models, the turbulent kinetic energy equation is modified through the addition of a dissipation term that is a function of the turbulent Mach number M_t. Initially designed for the $K-\epsilon$ model, these compressibility corrections have been successfully adapted and applied to other two-equation models, like the $K-\omega$ model.[13] Unfortunately, they are inapplicable to the one-equation models, as the Baldwin–Barth[14] and the Spalart–Allmaras[15] (S-A) models, because the lack of the turbulent kinetic energy as integration variable does not allow the computation of M_t. The absence of a compressibility correction significantly reduces the validity range of these models, which have displayed good performance in the computation of supersonic and hypersonic without free-shear regions.[16]

The present study proposes a compressibility correction to the S-A model that uses as a control parameter an estimate of M_c computed using the eddy viscosity ν_T and several local variables instead of M_t. This feature, which distinguishes the present correction from others, makes it suitable to be implemented in other turbulence models that do not integrate explicitly the turbulent kinetic energy.

Received 5 March 2002; revision received 8 January 2003; accepted for publication 16 January 2003.

*Research Scientist, Department of Mechanics and Aeronautics, Via Eudossiana 18. Member AIAA.
†Full Professor, Department of Mechanics and Aeronautics, Via Eudossiana 18.

The present paper outlines the development and validation of this correction. The correction was developed by modifying the original S-A model equation in order to "mimic" the compressibility effects inside the mixing layers. The correction has been validated through the simulations of mixing layers and by comparison against the available experimental data. Finally, to explore the validity of the compressibility correction in more complex flow geometries different supersonic flows over a backward-facing step have been computed, and their results have been compared against published experimental data.

Compressibility Effects in a Mixing Layer

Consider a mixing layer resulting from the merging of two parallel streams at two different freestream Mach numbers, as shown in Fig. 1. As already mentioned, the most visible effect of compressibility is the reduction of the mixing-layer growth rate with respect to an incompressible mixing layer having the same freestream velocity ratio r. Using the vorticity thickness δ_ω (Ref. 17) as measure of the mixing-layer thickness, the experimental measurements of the mixing-layer growth rate are well correlated by the following relation[5]:

$$\left(\frac{\mathrm{d}\delta_\omega}{\mathrm{d}x}\right) = C_\omega \frac{1-r}{1+r} \tag{1}$$

where C_ω is a nondimensional parameter depending mainly on M_c. For low-speed mixing layers at $M_c < 0.4$, $C_\omega = 0.168$, whereas C_ω decreases up to half this value when $M_c > 1$. For each mixing layer it is possible to define a normalized growth rate ratio based on the vorticity thickness:

$$\frac{(\mathrm{d}\delta_\omega/\mathrm{d}x)_c}{(\mathrm{d}\delta_\omega/\mathrm{d}x)_i} = \frac{(\delta_\omega)_c}{(\delta_\omega)_i} = \frac{C_\omega(M_c)}{C_\omega(0)} = f_1(M_c) \tag{2}$$

which relates the compressible flow thickness growth rate to that occurring in an incompressible mixing layer with the same r value by means of a function of M_c. This finding was demonstrated by Bogdanoff[9] using both theoretical arguments and experimental evidence.

As for the thickness growth rate, the compressibility effect on the turbulent shear stress can be described by a single function $f_2(M_c)$, which relates the dimensionless maximum shear stress

$$\tau = \frac{\overline{u'v'}|_{\max}}{\Delta U^2} \tag{3}$$

of a compressible mixing layer τ_c to that of the corresponding incompressible case τ_i, that is,

$$\tau_c = f_2(M_c)\tau_i \tag{4}$$

Under the self-preservation hypothesis[18] the nondimensional ratio τ_i can be assumed as a constant value for every incompressible mixing layer.

The functions f_1 and f_2, quantifying the effects of compressibility in the mixing layer, have been assumed as follows:

$$f_1(M_c) = 0.6\left[1\Big/\left(1+9M_c^6\right)\right] + 0.4 \tag{5}$$

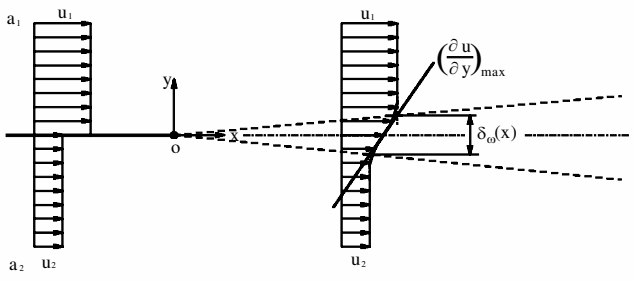

Fig. 1 Sketch of a mixing-layer flow.

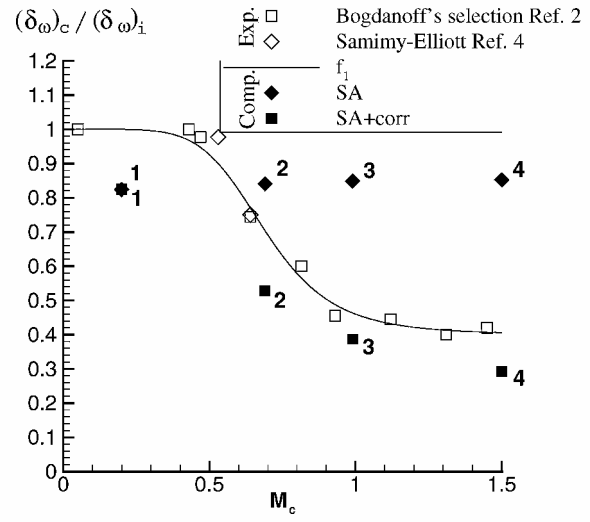

Fig. 2 Mixing-layer flow: experimental and numerical normalized vorticity thickness growth rate vs M_c.

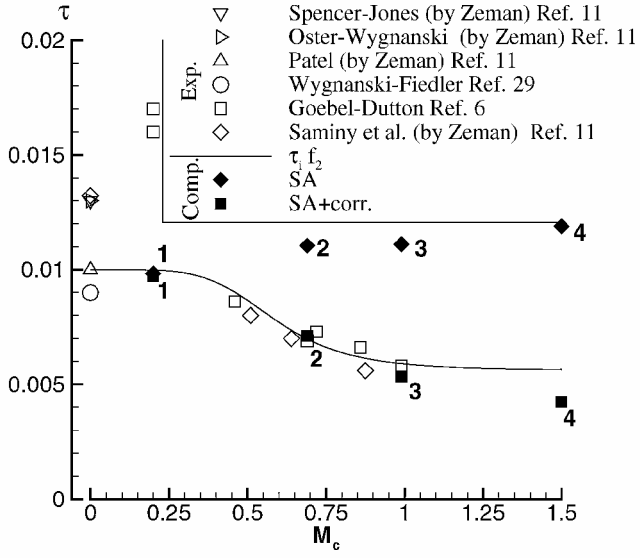

Fig. 3 Mixing-layer flow: experimental and numerical normalized maximum turbulent shear stress vs M_c.

$$f_2(M_c) = \left\{0.44\left[1\Big/\left(1+14M_c^5\right)\right] + 0.56\right\} \tag{6}$$

These expressions are based on a best fitting of the experimental data shown in Figs. 2 and 3.

Modeling of Compressibility Effects in the S-A Model

Figure 1 illustrates a simple mixing-layer flow. Under the assumption that the mixing layer is symmetric with respect to the x axis, the maximum velocity gradient $(\mathrm{d}u/\mathrm{d}y)_{\max}$, the maximum eddy viscosity value $\nu_{T\max}$, and the maximum turbulent shear stress $\overline{u'v'}|_{\max}$ take place along the x axis itself. Combining Eq. (4) with the Boussinesq closure and the vorticity thickness definition, it is possible to express the maximum eddy viscosity as

$$\nu_{T\max}(x) = \tau_i f_2(M_c)\Delta U \delta_\omega(x) \tag{7}$$

which, after differentiating with respect to x, becomes

$$\frac{\mathrm{d}\nu_{T\max}(x)}{\mathrm{d}x} = \tau_i f_2(M_c)\Delta U \frac{\mathrm{d}\delta_\omega(x)}{\mathrm{d}x} \tag{8}$$

From Eqs. (8) and (2) it is possible to obtain a relation that correlates the eddy viscosity growth rate in a compressible mixing layer to that

in an incompressible flow having the same velocities:

$$\left(\frac{\mathrm{d}v_{T\max}}{\mathrm{d}x}\right)_c = f_1(M_c) f_2(M_c)\left(\frac{\mathrm{d}v_{T\max}}{\mathrm{d}x}\right)_i \tag{9}$$

This relation shows that the compressibility reduces the growth rate of v_T in a mixing layer by a factor $f_1 \cdot f_2$. Therefore, multiplying by this factor the production term of the S-A equation, the model equation becomes

$$\frac{\mathrm{D}v_T}{\mathrm{D}t} = f_1(M_c) f_2(M_c)(c_{b1}|\omega| v_T) + \ldots \tag{10}$$

and the model is able to reproduce, as function of M_c, the same growth rate predicted by Eq. (9). Nevertheless, this correction is not yet general because it requires the a priori knowledge of the convective Mach number, which is often unknown in complex flows.

A generalization of this correction can be obtained if the convective Mach number M_c is replaced by its estimate $\tilde{M}_c$ computed on the basis of local quantities. Combining Eq. (7) with the vorticity thickness and the convective Mach-number definitions, it is possible to obtain an exact expression that relates M_c to $v_{T\max}$, $(\partial u/\partial y)_{\max}$, and the average of the freestream sound speeds:

$$M_c^2 f_2(M_c) = \frac{1}{4\tau_i}\frac{v_{T\max}(\partial u/\partial y)_{\max}}{[(a_1 + a_2)/2]^2} \tag{11}$$

Evaluating the right-hand side with the local variables, Eq. (11) becomes

$$\tilde{M}_c^2 f_2(\tilde{M}_c) = \frac{1}{4\tau_i}\frac{v_T|\omega|}{a^2} \tag{12}$$

This equation provides at every point of the flowfield a local estimate $\tilde{M}_c$ of the convective Mach number, which can be used in Eq. (10) instead of M_c. In other words, the variable $\tilde{M}_c$ plays here the same role of M_t in the corrections proposed by Zeman[11] or Sarkar et al.[12] However, unlike M_t, $\tilde{M}_c$ does not require the integration of the K equation because it is computed by means of Eq. (12) from the eddy viscosity and two local variables (ω and a).

Before concluding this section, it is worth pointing out an important issue concerning the boundary-layer flows. The velocity profile computed using the standard S-A model shows a noticeable displacement from the wall law for the compressible boundary layer when a large density variation occurs inside the boundary layer. Specifically, the presence of a density gradient inside the boundary layer modifies the equilibrium among the production, the destruction, and the diffusion term. The application of the present compressibility correction, which is valid for free shear flows, deteriorates further the behavior of the S-A model in boundary layers. Indeed for freestream Mach numbers larger than 5, high $\tilde{M}_c$ values can occur inside the compressible boundary layer, modifying significantly the production term determining a further alteration of the equilibrium. Similar problems were experienced also by other turbulence models and compressibility corrections, as reported by Huang et al.[19] The analysis of this interesting issue and the description of the possible remedies exceed the aims of this paper and will form the object of a specific study in a future work.

Verification, Validation, and Numerical Simulations

The compressibility correction has been implemented on a previously developed S-A solver. A detailed description of the integration method for the model equation can be found in Ref. 20. The S-A solver has been widely verified, coupled with several Reynolds-averaged Navier–Stokes formulation, and numerous test cases were computed, as documented in Refs. 7, 16, and 20–22. The compressibility correction has been added to the scheme by estimating the local convective Mach number from Eq. (12) with a Newton–Raphson method. In the present study all numerical results have been computed using the modified S-A solver coupled with a Godunov-type finite volume code.[23,24]

Table 1 Mixing-layer flows: test case definition

Parameter	1	2	3	4
M_c	0.2	0.69	0.99	1.5
r	0.78	0.18	0.16	0.11
M_1, M_2	2.01, 1.38	1.96, 0.27	2.27, 0.38	3.26, 0.38
T_1, T_2, K	163, 214	161, 281	332, 292	332, 292
p, KPa	46	53	32	32

Table 2 Coarse, medium, and fine computational mesh parameters

Level	Number of cells	Cells in strip	Δx	$\Delta y_{\min}$	$\Delta y_{\max}$
Coarse	40×60	25	0.05	0.006	0.2000
Medium	80×120	50	0.025	0.003	0.1000
Fine	160×240	100	0.0125	0.0015	0.0500

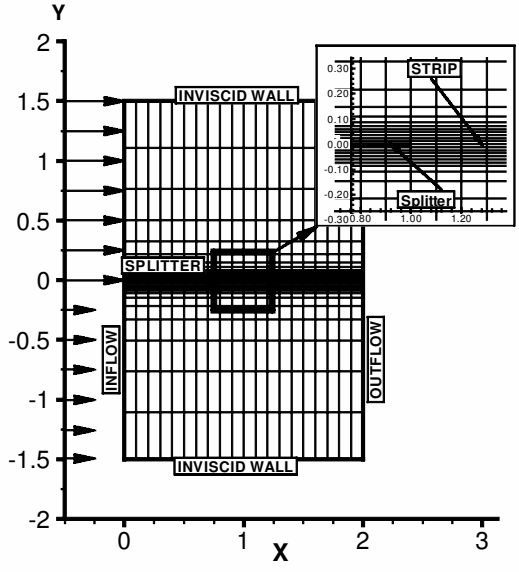

Fig. 4 Mixing-layer flow: computational domain, discretization grid, and boundary conditions.

Mixing-Layer Flows

Four mixing layers, where the compressibility has increasing importance, were selected. The convective Mach number of these flows, reported in Table 1 together with other inlet flow conditions, varies from $M_c = 0.2$ in the first case up to $M_c = 1.5$ in the last one. The test cases 1, 2, and 3 reproduce three experimental conditions studied by Goebel and Dutton in Ref. 6. The last case is obtained by varying the velocity flow of the high-speed stream of case 3, in order to increase the freestream Mach number and, consequently, the convective Mach number.

The computational domain is a rectangular area (Fig. 4), with a splitter plate separating the high-speed from the low-speed region for half the length of the computational domain. This way, the mixing-layer region is not influenced by the inflow boundary. The influence of the lower and upper boundaries on the prediction has also been minimized by defining a domain height at least 30 times larger than the maximum mixing-layer thickness. Along the inflow boundary a subsonic or supersonic inflow condition is imposed according to the freestream Mach number. Specifically, where the inflow Mach number is subsonic, the velocity direction, the total pressure, and the total temperature are assigned together with a constant eddy viscosity profile with $v_T/v = 0.1$. Where the Mach number is supersonic, a constant profile is imposed of all variables. Along the outflow boundary the flow state is extrapolated where the exit Mach number M_e is supersonic, else the external pressure is imposed where $M_e < 1$. Finally, along both sides of the splitter plate and at the upper and lower boundaries, the inviscid wall condition is applied. Numerical computations have been performed using three meshes of increasing level of refinement, detailed in Table 2.

Table 3 Predictions of the vorticity thickness spread rate and the maximum shear stress and GCI

	$d\delta_\omega/dx$		τ	
Test case	SA	SA + correction	SA	SA + correction
1	0.01711 ± (0.00015)	0.01708 ± (0.00018)	0.00983 ± (0.00032)	0.00973 ± (0.00044)
2	0.09812 ± (0.00198)	0.06118 ± (0.00021)	0.01105 ± (0.00016)	0.00711 ± (0.00006)
3	0.10324 ± (0.00075)	0.04726 ± (0.00119)	0.01110 ± (0.00008)	0.00534 ± (0.00009)
4	0.11480 ± (0.00113)	0.03941 ± (0.00231)	0.01188 ± (0.00010)	0.00425 ± (0.00010)

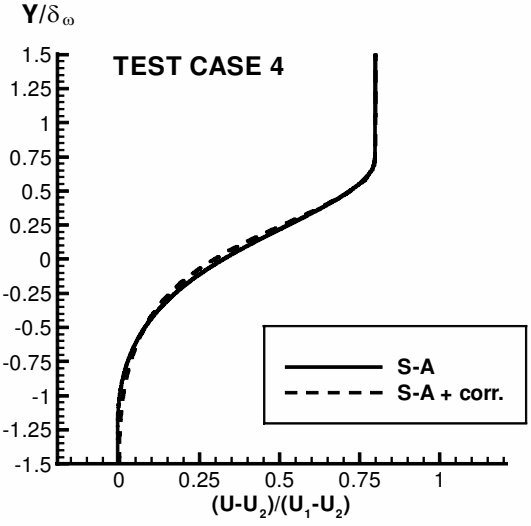

Fig. 5 Similarity profile of normalized mean streamwise velocity for test case 4.

The evaluation of the numerical errors was carried out by means of the computation of the grid convergence index (GCI). This index, proposed by Roache,[25] provides an error bandwidth for the numerical predictions and requires the computation of numerical solutions on at least two discretization levels. For each test case the computations have been performed decreasing the mesh size until the GCI was less than 5% of the predicted value.

To evaluate the effectiveness of the compressibility correction, each test case has been computed both with and without the correction. The predicted thickness growth rate and the maximum shear stress are reported in Table 3 together with the corresponding GCI values.

Despite the influence on $d\delta_\omega/dx$ and τ, the compressibility correction does not alter the shape of the similarity velocity profile. As shown in Fig. 5, the compressibility correction introduces only minimal difference, even in the case of the larger convective Mach number (test case 4).

Figure 2 shows the computed vorticity thickness growth rates and corresponding experimental data at varying M_c. The experimental measurements of different authors[17,26–28] selected by Bogdanoff[2] are indicated by hollow squares, and two additional measurements by Samimy and Elliot[4] are denoted by hollow diamonds. Both the numerical and experimental data are normalized with respect to the corresponding incompressible vorticity thickness growth rate predicted by Eq. (1).

When M_c is small, as in test case 1, the compressibility effects are negligible, and the results obtained by the standard and by the corrected model practically coincide. The compressibility correction is not responsible for the numerical prediction underestimate of test 1, the origin of which has to be found in the behavior of the standard S-A model.

As M_c increases (test cases 2, 3, and 4) the growth rate predicted by the standard S-A model remain constant. This indifference to M_c is not a common property of all turbulence models deprived of a compressible modeling. For instance, the growth rates predicted by the standard $K-\varepsilon$ model exhibit, as M_c increases, a slight decrease,[5] which, by itself, is not sufficient to reproduce the experimental behavior.

Table 4 Nominal and estimated convective Mach number

Test case	M_c	$\tilde{M}_{c\,\max}$	$T_{\max}/\max(T_1, T_2)$
1	0.2	0.2	1.0
2	0.69	0.677	1.0
3	0.99	0.83	1.12
4	1.5	1.05	1.35

The thickness growth rates computed with the corrected S-A model reproduce the experimental decrease, even though a general underestimate is observed. Of course, a recalibration of the standard model improving the prediction of the thickness growth rate in the incompressible case could improve even the compressible predictions.

Concerning the maximum shear stress, shown in Fig. 3, a brief justification about the choice of the expression of f_2 is needed before proceeding to the comparison between the experimental and the numerical data. This expression is somehow influenced by the choice of the τ_i value. Indeed, the experimental data show a wide dispersion of the shear-stress values at low M_c, whereas as M_c increases the experimental dispersion is smaller. Specifically, the dimensionless stress in the incompressible mixing layers ranges from the value 0.017 measured by Goebel and Dutton[6] to the value 0.009 observed by Wygnanski and Fiedler.[29] Actually, the uncertainty bandwidth should be less because the measurements of Goebel and Dutton have been probably obtained in mixing layers not completely developed.[30] In general, the choice of a specific τ_i value inside this interval implies a specific expression for f_2 in order to match the experimental data at high M_c. In the case of the S-A model, the choice of the τ_i value is dictated by the original model calibration that assumes $\tau_i = 0.01$. As can be seen in Fig. 3, the f_2 expression of Eq. (6) is compatible with such a value of τ_i. Even for the maximum shear stress, the comparison between the experimental and the numerical data shows that the model without correction predicts values slightly increasing with M_c, whereas the corrected model predictions are in good agreement with the experimental data.

Before concluding the analysis of mixing-layer solutions, it is worth evaluating the reliability of the convective Mach-number estimate provided by Eq. (12). In the proximity of the mixing-layer longitudinal axis, $\tilde{M}_c$ reaches a maximum value that remains constant along the whole mixing layer. Such maximum should be approximately equal to the nominal convective Mach number. Table 4 shows that $\tilde{M}_{c\,\max}$ sometimes underestimates the nominal values (test cases 3 and 4). This misprediction can be related to the presence of a peak in the temperature profile caused by the kinetic energy dissipation. In fact, when the temperature peak occurs $[T_{\max} > \max(T_1, T_2)]$, the denominator of Eq. (12) overpredicts that of Eq. (11) as the local sound speed is greater than the average of the freestream ones. The temperature peak in a mixing layer depends on the difference between the freestream temperatures and on the strength of the mechanical dissipation. $T_{\max}$ is therefore higher at increasing convective Mach numbers. Still, at $M_c > 1.0$ the dependence on M_c of the compressibility effects becomes weaker, as indicated by the experimental data reported in Figs. 2 and 3. Therefore, a misprediction of M_c does not produce significant errors, as shown by the computations of test case 4.

Supersonic Axisymmetric Base Flows

The supersonic backward-facing step flow is an interesting application, where compressibility effects have a great influence on the

base pressure. A schematic view of this flow in Fig. 6 shows that, even if the body geometry is very simple such as with a cylindrical afterbody, the flow structure is quite complex. The flowfield is mainly composed of an inviscid outer region and a turbulent inner recirculating region. The former is a supersonic region characterized by a strong expansion centered at the corner, followed by compression waves coalescing in a shock near the flow reattachment point. The inner region is dominated by a low-speed flow with nearly constant pressure. The two regions are connected through a turbulent free shear layer originating at the edge. The turbulent mixing and the energy exchange between the inner and outer regions are critical in determining the base pressure. For this reason, a strict relationship exists between the Mach number at the base shoulder and the base pressure. (See Ref. 7 for a more detailed explanation of this relationship.)

Four different flow conditions with increasing values of the freestream Mach number ($M_1 = 1.1, 1.6, 2.46, 3.39$) have been considered. The third test case corresponds to the experimental conditions of Herrin and Dutton.[31] For each test case the computation has been performed on two orthogonal grids of increasing spatial resolution (80×106, 160×212) generated by means of a conformal mapping transformation,[32] as shown in Fig. 7. As in mixing-layer computations, the errors of the numerical solutions have been estimated by the GCI method. Table 5 reports the average base pressure normalized by the freestream pressure and computed with either turbulence model on the finest discretization level. Each value is followed by its GCI, which is in all cases less than 10% of the average pressure value.

The results of Table 5 show that the compressibility correction yields a generalized increase of the average base pressure, starting from 10%, when the Mach number is low ($M_\infty = 1.1$) up to a 90% increment at the highest Mach number ($M_\infty = 3.39$), where the compressibility effects are stronger.

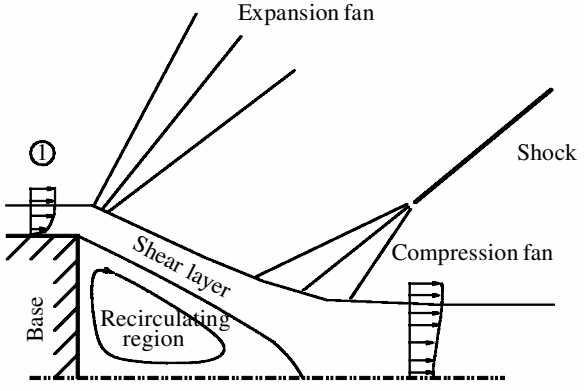

Fig. 6 Sketch of a supersonic base flow.

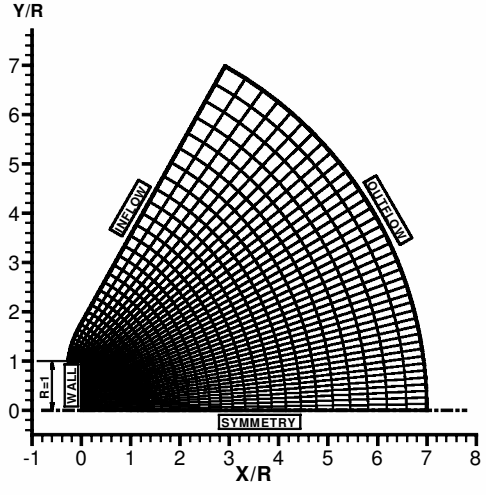

Fig. 7 Supersonic base flow: computational domain, discretization mesh, and boundary condition.

Table 5 Supersonic base flow: normalized averaged base pressure and GCI

M_∞	Standard S-A	S-A + correction
1.1	$0.748 \pm (0.041)$	$0.815 \pm (0.067)$
1.6	$0.509 \pm (0.006)$	$0.645 \pm (0.023)$
2.46	$0.276 \pm (0.007)$	$0.475 \pm (0.041)$
3.39	$0.148 \pm (0.001)$	$0.280 \pm (0.022)$

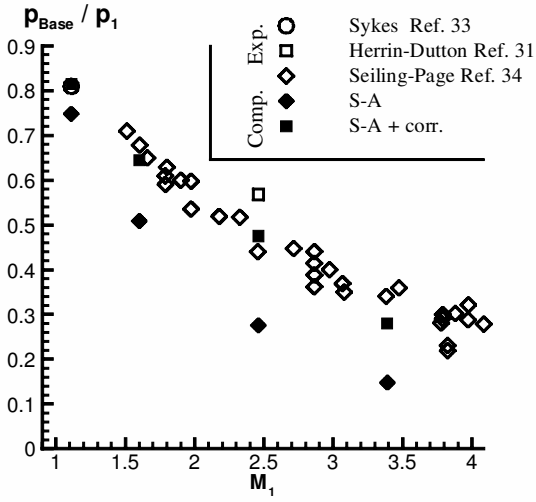

Fig. 8 Averaged base pressure vs the Mach number M_∞.

The numerical predictions of the base pressure are compared in Fig. 8 with the available experimental measurements of Sykes,[33] Herrin and Dutton,[31] and of Seiling and Page.[34] The corrected model provides estimates that fit well the experimental trend and are always inside the dispersion bandwidth, whereas the standard model provides estimates with large errors, which, at the higher Mach number, are about 100% of the predicted value.

Conclusions

The compressibility correction proposed for the Spalart–Allmaras (S-A) model has provided promising results. The numerical simulations have proven that the correction is able to account for compressibility effects both in simpler flow configurations and in more complex ones. The application of this correction to the S-A model significantly extends the model validity to compressible flows. Moreover, the characteristics of the present correction give scope for further advances in the field of turbulence modeling. Indeed, the proposed compressibility correction could be adapted to other turbulence models that do not integrate the turbulent kinetic energy equation.

Acknowledgments

This work was supported by MIUR, the Italian Ministry of Education, University and Research. The authors are grateful to Aldo Rona, University of Leicester, who reviewed the manuscript.

References

[1] Lele, S. K., "Compressibility Effects on Turbulence," *Annual Review of Fluid Mechanics*, Vol. 26, 1994, pp. 211–254.

[2] Bogdanoff, D. W., "Compressibility Effects in Turbulent Shear Layer," *AIAA Journal*, Vol. 21, No. 6, 1983, pp. 926, 927.

[3] Papamoschou, D., and Roshko, A., "The Compressible Turbulent Shear Layer: an Experimental Study," *Journal of Fluid Mechanics*, Vol. 197, Dec. 1988, pp. 453–477.

[4] Samimy, M., and Elliott, G. S., "Effects of Compressibility on the Characteristics of Free Shear Layers," *AIAA Journal*, Vol. 28, No. 3, 1990, pp. 439–445.

[5]Viegas, J. R., and Rubesin, M. W., "Assessment of Compressibility Corrections to the $k-\varepsilon$ Model in High-Speed Shear Layers," *AIAA Journal*, Vol. 30, No. 10, 1992, pp. 2369, 2370.

[6]Goebel, S. G., and Dutton, J. C., "Experimental Study of Compressible Turbulent Mixing Layers," *AIAA Journal*, Vol. 29, No. 4, 1991, pp. 538–546.

[7]Paciorri, R., Nasuti, F., and Sabetta, F., "Evaluation of Turbulence Modeling in Supersonic Afterbody Computations," AIAA Paper 2001-3039, June 2001.

[8]Tucker, P. K., and Shyy, W., "A Numerical Analysis of Supersonic Flow over an Axisymmetric Afterbody," AIAA Paper 93-2347, June 1993.

[9]Sahu, J., "Numerical Investigation of Supersonic Base Flow with Base Bleed," *Journal of Spacecraft and Rockets*, Vol. 34, No. 1, 1997, pp. 62–69.

[10]Ottens, H. B. A., Gerritsma, M. I., and Bannink, W. J., "Computational Study of Support Influence on Base Flow of a Model in Supersonic Flow," AIAA Paper 2001-2638, June 2001.

[11]Zeman, O., "Dilatation Dissipation: The Concept and Application in Modeling Compressible Mixing Layer," *Physics of Fluids A*, Vol. 2, No. 2, 1990, pp. 178–187.

[12]Sarkar, S., Erlebacher, G., Hussaini, M. Y., and Kreiss, H. O., "The Analysis and Modelling of Dilatational Terms in Compressible Turbulence," *Journal of Fluid Mechanics*, Vol. 227, June 1991, pp. 473–493.

[13]Wilcox, D. C., *Turbulence Modeling for CFD*, DCW Industries, La Cañada, CA, 1993, Chap. 5.

[14]Baldwin, B. S., and Barth, T. J., "A One-Equation Turbulence Transport Model for High Reynolds Number Wall-Bounded Flows," AIAA Paper 91-0610, Jan. 1991.

[15]Spalart, P. R., and Allmaras, S. R., "A One-Equation Turbulence Model for Aerodynamic Flows," *La Recherche Aérospatiale*, No. 1, 1994, pp. 5–21 (in English).

[16]Paciorri, R., Dieudonné, W., Degrez, G., Charbonnier, J.-M., and Deconinck, H., "Exploring the Validity of the Spalart–Allmaras Turbulence Model for Hypersonic Flows," *Journal of Spacecraft and Rockets*, Vol. 35, No. 2, 1998, pp. 121–126.

[17]Brown, G. L., and Roshko, A., "On Density Effects and Large Structure in Turbulent Mixing Layers," *Journal of Fluid Mechanics*, Vol. 64, July 1974, pp. 775–816.

[18]Tennekes, H., and Lumley, J. L., *A First Course in Turbulence*, MIT Press, Cambridge, MA, 1972, Chap. 4.

[19]Huang, P. G., Bradshaw, P., and Coakley, T. J., "Turbulence Models for Compressible Boundary Layers," *AIAA Journal*, Vol. 32, No. 4, 1994, pp. 735–740.

[20]Paciorri, R., Deconinck, H., and Degrez, G., "Implementation and Validation of the Spalart-Allmaras Turbulence Model for Application in Hypersonic Flows," von Kármán Inst., TN-190, Sint-Genesius-Rode, Belgium, Jan. 1996.

[21]Di Mascio, A., Paciorri, R., and Favini, B., "Truncation Error Analysis in Turbulent Boundary Layer," *Journal of Fluid Mechanics*, Vol. 124, Sept. 2002, pp. 657–663.

[22]Nasuti, F., Paciorri, R., and Onofri, M., "Computation of Turbulent Supersonic Base Flows by a Shock Fitting Quasi-Linear Solver," American Society of Mechanical Engineers, Paper FEDSM99-7316, July 1999.

[23]Di Mascio, A., and Favini, B., "A Two-Step Godunov-Type Scheme for the Euler Equation," *Meccanica*, Vol. 26, No. 2–3, 1991, pp. 179–188.

[24]Favini, B., Broglia, R., and Di Mascio, A., "Multigrid Acceleration of Second Order ENO Schemes from Low Subsonic to High Supersonic Flows," *International Journal for Numerical Methods in Fluids*, Vol. 23, No. 6, 1996, p. 589.

[25]Roache, P. J., "Quantification of Uncertainty in Computational Fluid Dynamics," *Annual Review of Fluid Mechanics*, Vol. 29, 1997, pp. 123–160.

[26]Ikawa, H., and Kubota, T., "Investigation of Supersonic Turbulent Mixing Layer with Zero Pressure Gradient," *AIAA Journal*, Vol. 13, No. 5, 1975, pp. 566–572.

[27]Maydew, R. C., and Reed, J. F., "Turbulent Mixing of Compressible Free Jets," *AIAA Journal*, Vol. 1, No. 6, 1963, pp. 1443, 1444.

[28]Sirieux, M., and Solignac, J.-L., "Contribution a l'Etude Experimentale de la Couche de Melange Turbulent Isobare d'un Ecoulement Supersonique," *Symposium on Separated Flow, AGARD Conference Proceedings*, No. 4, 1966, pp. 241–270 (in French).

[29]Wygnanski, I., and Fiedler, H., "The Two-Dimensional Mixing Region," *Journal of Fluid Mechanics*, Vol. 41, April 1970, pp. 327–361.

[30]Barre, S., Quine, C., and Dussauge, J. P., "Compressibility Effects on the Structure of Supersonic Mixing Layers: Experimental Results," *Journal of Fluid Mechanics*, Vol. 259, Jan. 1994, pp. 47–78.

[31]Herrin, J. L., and Dutton, J. C., "Supersonic Base Flow Experiments in the Near Wake of a Cylindrical Afterbody," *AIAA Journal*, Vol. 32, No. 1, 1994, pp. 77–83.

[32]Nasuti, F., Onofri, M., and Valorani, M., "Orthogonal Grid Generation for Internal Flows by Conformal Mapping," *Numerical Methods in Laminar and Turbulent Flow*, Vol. 8-1, edited by C. Taylor, Pineridge Press, Swansea, Wales, U.K., 1993, pp. 1359–1369.

[33]Sykes, D. M., "Cylindrical and Boat-Tailed After-Bodies in Transonic Flow with Gas Ejection," *AIAA Journal*, Vol. 8, No. 3, 1970, pp. 588–590.

[34]Seiling, W. R., and Page, R. H., "A Re-Examination of Sting Interference Effects," AIAA Paper 70-585, May 1970.

T. C. Lin
Associate Editor